

Models of Fractal River Basins

Marek Cieplak,¹ Achille Giacometti,² Amos Maritan,³ Andrea Rinaldo,⁴
Ignacio Rodriguez-Iturbe,⁵ and Jayanth R. Banavar⁶

Received July 24, 1997; final January 16, 1998

Two distinct models for self-similar and self-affine river basins are numerically investigated. They yield fractal aggregation patterns following nontrivial power laws in experimentally relevant distributions. Previous numerical estimates on the critical exponents, when existing, are confirmed and superseded. A physical motivation for both models in the present framework is also discussed.

KEY WORDS: Dynamical critical phenomena; growth process; rivers; runoff and stream flow; erosion and sedimentation; aggregation patterns.

I. INTRODUCTION

Experimental analyses of river networks⁽¹⁾ have shown clear examples of behavior analogous to critical phenomena characterized by the absence of a single well-defined length scale reflected in a power-law behavior of various quantities. A fundamental question that arises from these observations is whether, in analogy with conventional critical phenomena, one may fruitfully classify this behavior into universality classes that are characterized by different sets of exponents. A related point is whether there exist scaling relationships between the various exponents of a given universality class. Another vital issue is the elucidation of simple models amenable to

¹ Polish Academy of Science, 02-668 Warsaw, Poland.

² INFN Unità di Venezia, Dipartimento di Scienze Ambientali, I-30123 Venice, Italy.

³ INFN Trieste and International School for Advanced Studies (SISSA), I-34014 Grignano di Trieste, Italy.

⁴ Istituto di Idraulica "G. Poleni," Università di Padova, I-35131 Padua, Italy.

⁵ Department of Civil Engineering, Texas A&M University, College Station, Texas 77843.

⁶ Department of Physics and Center for Materials Physics, Pennsylvania State University, 104 Davey Laboratory, University Park, Pennsylvania 16802.

analysis that nevertheless capture some of the features of fractal fluvial patterns.

Within this framework a theoretical description of the system needs to address two basic issues.⁽²⁻⁹⁾ First, a careful characterization of the *topological* properties of the networks is essential for understanding the basic transport mechanism in the basin. References 2 and 3 are recent attempts in this direction. Optimization principles have been exploited both numerically^(4, 7) and analytically⁽⁵⁾ to explain the tendency of natural drainage networks to evolve toward an optimal stable topology. General scaling arguments can be found in ref. 8.

Second, a study of the dynamical evolution of the landscape (on geological time scales) as a result of interaction with external agents (rain, wind etc.) would be desirable.^(6, 9)

The present work will address only the first point. We will argue that, despite much progress in the past few years, the problem is not yet fully understood and deserves further analysis. To this aim we will discuss, based on physical arguments, two toy models of river networks. The first model leads to a *self-similar* river basin, and is relevant when the erosional properties of the surface soil are strongly heterogeneous. The second model considers the homogeneous basin case and results in a self-affine river network.

Although the overwhelming majority of the observational data are consistent with a *self-affine* description (i.e., networks display a privileged direction), the marked self-similarity of the basins with their own sub-basins suggests a crossover from a *self-similar* character above some length scale. This is one of the reasons for considering models with both characters. It should also be emphasized that although some of the features of the models presented here were previously discussed in the literature (see below), we believe that both the physical motivations and the analysis carried out here are essentially new.

The plan of the paper is as follows. In the next section few definitions and scaling relations will be recalled. In Section III results for self-similar are presented. Section IV is dedicated to the self-affine counterpart. In Section V few relevant experimental results will be briefly reminded for the sake of completeness. Section VI will summarize our findings along with some future perspectives.

II. DEFINITIONS AND SCALING LAWS

We define a river network as a spanning (loopless) tree on a lattice of linear size L .⁽¹⁰⁾ Each site has exactly one output bond to one of its neighbors and no restriction on the number of input bonds (three at most

on a square lattice). In a river basin, the area at any site is defined as the number of sites upstream of the site connected by the network. From the computational point of view, it can also be regarded as a measure of the flow rate if a unit weight is assigned to each source thus simulating a unit constant precipitation.

The equation for s_i , the area at a given site i , is

$$s_i = \sum_{j \in nn(i)} w_{ij} s_j + 1 \quad (1)$$

where w_{ij} is 1 if i collects water from its nearest-neighbor (nn) site j and 0 otherwise.

It is experimentally observed⁽¹⁾ and theoretical explained^(7,8) that in river basins the probability density $p(s, L)$ of a site having area s in a system of size L , has the scaling form

$$p(s, L) = s^{-\tau} F\left(\frac{s}{L^\phi}\right) \quad (2)$$

where $F(x)$ is a scaling function which takes into account finite size effects and ϕ is the finite size exponent.

Similarly the distribution of *upstream* lengths has been also predicted⁽⁸⁾ and confirmed by field observation⁽¹¹⁾ to display the universal form:

$$\pi(l, L) = l^{-\gamma} f\left(\frac{l}{L^{d_l}}\right) \quad (3)$$

where $f(x)$ is the analogue of $F(x)$ and d_l coincides with the stream fractal dimension. The upstream length is defined as follows. At a given site the areas (see Eq. (1)) of the nearest-neighbours are checked. The site with the largest value leads to the outlet. The site with the next-largest value is defined to be an upstream site—it indicates the longest path towards the source. If two (or more) equal areas are encountered, one is randomly selected. Alternatively, a burning algorithm⁽³⁾ could be also employed.

In natural basins, the drainage area s and the stream length l are related by Hack's law⁽¹²⁾

$$s \sim l^{1/h} \quad (4)$$

The sub-basin from any site defined as all the upstream sites connected to it is characterized by typical longitudinal and transverse lengths $\xi_{||}$ and ξ_{\perp} . For self-affine river networks one defines the Hurst (or wandering) exponent as $\xi_{\perp} \sim \xi_{||}^H$ with $H \leq 1$. Note that for self-similar river networks

(in which each rivulet originating from any site and proceeding to the global outlet is a fractal characterized by the same fractal dimension d_l), the Hurst exponent $H = 1$.

As one might expect the exponents are not independent. For *self-similar* networks ($d_l > 1$, $H = 1$) d_l determines all the other exponents^(7, 8)

$$\phi = 2, \quad h = d_l/2, \quad \tau = 2 - 2/d_l, \quad \gamma = 2/d_l \quad (5)$$

For *self-affine* networks ($d_l = 1$, $H < 1$) it is H which defines all the other exponents⁽⁵⁾

$$\phi = 1 + H, \quad h = 1/(1 + H), \quad \tau = \frac{1 + 2H}{1 + H}, \quad \gamma = 1 + H \quad (6)$$

Two features of the above relations are worth mentioning. First there is experimental evidence in the observed data that $H < 1$ and $d_l > 1$. This apparent contradiction might be explained with the crossover between the two regimes occurring at some length scale, as mentioned in the introduction. Secondly it turns out from (5) and (6) that *identical* values of the exponents are obtained from both cases if $d_l = 2/(1 + H)$. This means that knowledge of the exponents other than d_l and H cannot discriminate the self-similar or self-affine character of the basin. In this respect a direct measure of d_l and H appears to be crucial for its characterization.

III. SELF-SIMILAR RIVER NETWORK MODEL

We first discuss the model of *self-similar* river networks. Consider a network which is a square lattice of size $L \times L$ where the links of the rivers are identified with the bonds of the lattice. Periodic boundary conditions are assumed in the left-right direction. The bottom side of the square is defined to be the (fixed) outlet which collects the water that is flowing out. Independent random numbers in the range $(0, 1)$ are assigned to the different bonds representing the erodability P'_i s, of the surface soil of the bond i .

The physical situation we have in mind leads to river network formation based on an invasion percolation like mechanism.⁽¹³⁾ The weakest erodable link is selected and assumed to be a part of the network. The second-ranking weakest link is then selected and so on. The process is iterated in the ensemble of the remaining links until all sites are connected, i.e., they all have a route to the outlet. Loops are excluded since once a preferred route is selected, alternative routes formed due to the presence of a loop would be energetically unfavourable. Operationally, one thus obtains the network by incorporating the regions in order of increasing

strength so that no loops are formed, yet all sites on the lattice are connected to the outlet sites. A variant of the above procedure leading to the same structure, consists of starting from the links connected to the outlets, selecting the weakest one and proceeding invasively (i.e., always choosing the new weakest link) in the new ensemble of the interfacial links. This model, which was originally introduced by Stark⁽²⁾ was subsequently rediscovered by Manna and Subramanian.⁽³⁾ This is a model of headward growth of streams away from a rift, the weakest bond corresponding to the point most susceptible to bank failure. The motivations which led the above authors to the model were however completely different from ours. One might suspect that a variant of the above model having (statistically) spherical geometry would lead to a different universality class. We checked that this is *not* the case by starting with a central outlet and proceeding as above until the whole domain is drained.

A typical river obtained by our procedure is shown in Fig. 1. We have carried out detailed studies of the scaling properties of the networks. Our numerical simulations involved sizes up to $L = 192$ with a typical number

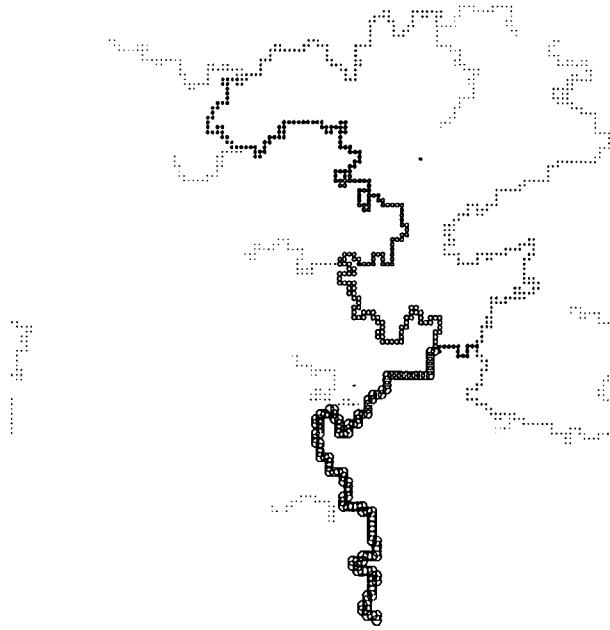


Fig. 1. Typical self-similar river network on a 128×128 lattice obtained by our optimization procedure. Only the largest river is shown. Periodic boundary conditions are used only in the direction transverse to the dominant flow. The size of the circles is a measure of the value of s .

of different configurations of the order of 500. A summary of our results is presented in Table I along with the results of observational data.⁽¹⁾ In order to get a precise estimate of the τ exponent we used two different methods. The first consists in plotting the local slope (which is trivially related to τ) of the cumulate area distribution (see Fig. 2)

$$P(s, L) = \int_0^s ds' p(s', L) \quad (7)$$

as a function of s . This is reported in Fig. 3. An average over all these values yields $\tau = 1.406 \pm 0.021$. On the other hand we performed a finite size analysis of the exponent extracted at the various sizes (see Fig. 4). An extrapolation then yields $\tau = 1.404 \pm 0.001$. The value reported in Table I is then the arithmetic average of these two values. The exponent ϕ can be determined by plotting the universal function as defined in (2). This is also shown in Fig. 5. In a similar way we computed the exponent γ as defined in (3) obtaining $\gamma = 1.612 \pm 0.049$. In Fig. 6 the universal function $f(x)$ is computed yielding a good collapse for $d_f = 1.22$. The value for d_f can be confirmed by an independent computation of the typical length

$$\frac{\langle l^q \rangle}{\langle l^{q-1} \rangle} = L^{d_f} \quad (8)$$

Table I. The Exponents Predicted by the Scaling Arguments, Measured in Our Simulations and for River Basins^a

	Self-similar		Self-affine		River basins
	Scaling predictions (with $d_f = 1.21 \pm 0.02$)	Measured	Scaling predictions (with $H = \frac{2}{3}$)	Measured	
d_f	1.21 ± 0.02	1.22 ± 0.04	1	1	1.1 ± 0.2
H	1	1	$\frac{2}{3}$	—	0.75–0.80
τ	1.395 ± 0.01	1.38 ± 0.03	$\frac{7}{5}$	1.40 ± 0.02	1.43 ± 0.02
h	0.605 ± 0.01	0.62 ± 0.02	$\frac{2}{3}$	—	0.57–0.60
γ	1.65 ± 0.03	1.60 ± 0.05	$\frac{5}{3}$	—	1.8–1.9
d_F	1.21 ± 0.02	1.21 ± 0.02	1	1	—

^a d_F is the fractal dimension of the river basin boundary. Note the inconsistency in the observational data— d_f is greater than 1 suggesting a self-similar network, whereas $H < 1$ indicating a self-affine structure.

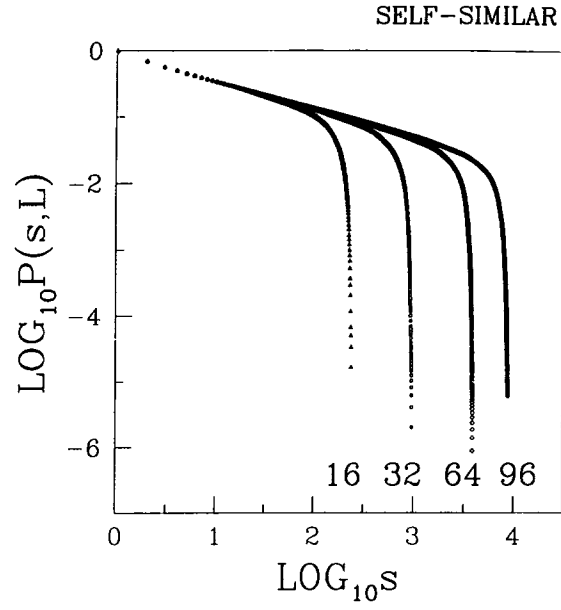


Fig. 2. A log-log plot of the cumulate area distribution $P(s, L)$ vs. s , for lengths ranging from $L=16$ to $L=96$. The value of the exponent $\tau = 1.395 \pm 0.01$ can be compared with $\tau = 1.33$ corresponding to the Scheidegger and $\tau = 1.5$ corresponding to the Mean Field model.⁽¹⁴⁾

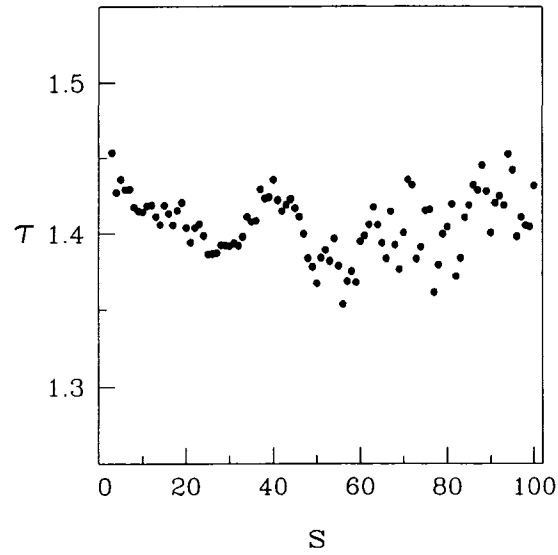


Fig. 3. Effective exponent τ as computed from the local slope.

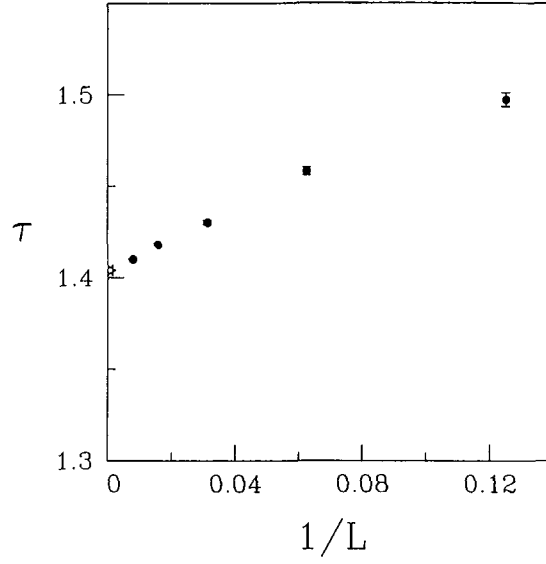


Fig. 4. Plot of the exponent τ as a function of $1/L$. The extrapolated value is $\tau = 1.404 \pm 0.001$ is indicated by a star.

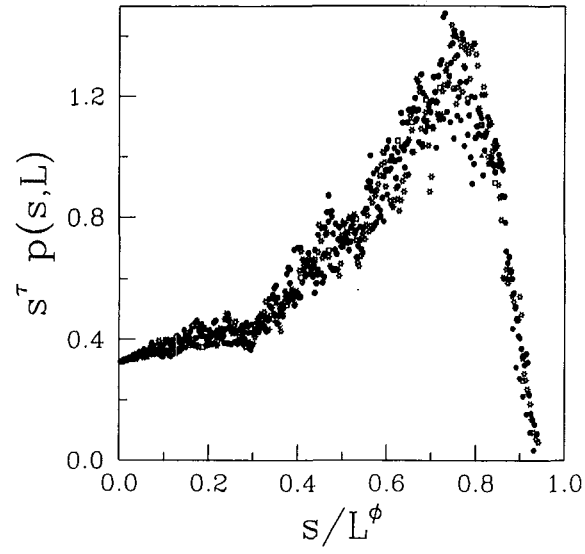


Fig. 5. Collapse of the $p(s, L)$ curves for $L=8$ (solid diamonds), 16 (boxes), 32 (solid hexagons), 64 (stars), and 96 (closed circles) according to Eq. (2), with $\tau = 1.40$ and $\phi = 2.0$.

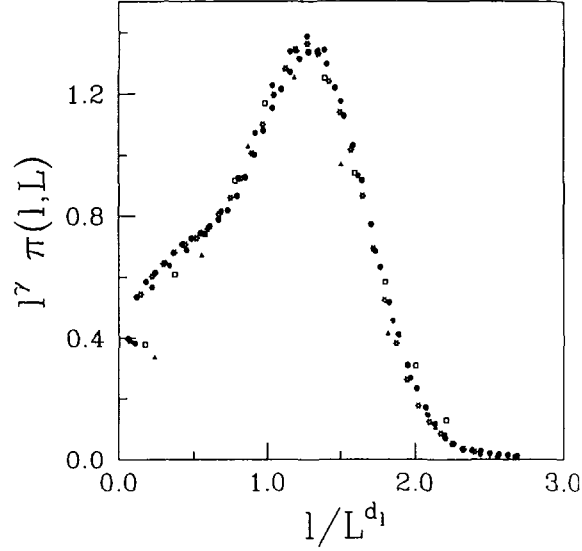


Fig. 6. Plot of the universal function $f(x)$ obtained from Eq. (3) for the same values as in Fig. 5) with $\gamma = 1.61$ and $d_l = 1.22$.

where the averages are referred to the probability distribution density $\pi(l, L)$. Using various values of q we found stable values allowing an estimate as $d_l = 1.22 \pm 0.05$.

The scaling predictions are found to hold very well. Our exponents agree with those numerically obtained recently in ref. 3. Specifically they reported $\tau = 1.392 \pm 0.010$ and $\gamma = 1.628 \pm 0.05$, upon using sizes up to $L = 1024$ but with a less precise data analysis.

This model may be alternately viewed as an optimization problem that selects the spanning tree that minimizes $\sum_i P_i$ where P_i denotes the erodability of the i th bond and the sum over i runs over all the bonds of the tree.^(5, 15) Our model then becomes a special case of the recently introduced optimal channel networks^(4, 7) that are constrained to satisfy a global minimization of the energy expenditure.⁽¹⁶⁾

We note that the resulting network is a union of the invasion percolation paths from each of the sites to the outlet.⁽¹⁷⁾ We also note that when two paths intersect, they coincide the rest of the way to the outlet. This provides a natural mechanism for aggregation in our model. Also each of the individual paths corresponds to the optimal path in a strongly disordered medium that was recently shown⁽¹⁸⁾ to be characterized by $d_l = 1.21 \pm 0.02$. Note that this value is somewhat different from the value 1.13 cited by Stark.⁽²⁾ That value corresponds to the fractal dimension of the *geometrical*

shortest path on a percolation cluster and is different from the fractal dimension of the loopless strands which correspond to the *energetically* shortest path in the sense explained above.

The Hurst exponent H obtained⁽¹⁹⁾ from a box-counting dimension d_I would be $2 - d_I$ and thus in the range 0.77–0.81. With this value of H and using the scaling relations in the text, we obtain $\tau = 1.44 \pm 0.04$, $h = 0.56 \pm 0.01$, and $\gamma = 1.79 \pm 0.02$ in perfect agreement with the observational data. Such a crossover might occur at some intermediate length scale beyond which the rivers are no longer self-similar.

We note that the homogeneous analog of our optimal channel network ($P_i = \text{const}$) is the random spanning tree problem, in which all trees occur with equal probability, $d_I = 5/4$ and the other exponents follow from our scaling relationships.⁽¹⁰⁾ Our model seems to be in a different universality class presumably due to the distinct weights associated with the different trees. The possibility that our result of $d_I \approx 1.21$ may crossover to $5/4$ for much larger sizes cannot of course be ruled out from our data.⁽²⁰⁾

IV. SELF-AFFINE RIVER NETWORK MODEL

We now turn to the second model leading to self-affine ($H < 1$) river networks. This corresponds to the homogeneous version of the first model where the P_i 's are all equal. Now the interfacial links all have an equal probability of being invaded with the usual constraint that loops are not formed. This procedure is akin to the well-known Eden growth problem. A loopless cluster generated in a two-dimensional Eden growth process on a square lattice with a central seed site is shown in Fig. 7. This model is not new. Meakin⁽²¹⁾ numerically studied the same model although with different aims. By mapping this problem onto a $1 + 1$ Kardar-Parisi-Zhang equation, Krug and Meakin⁽²²⁾ realized that the value $\tau = 1.40$ should be exact. As argued in refs. 23, the individual rivers are no longer self-similar but self-affine with a Hurst exponent of $2/3$. The Hurst exponent is larger than the random walk value of $\frac{1}{2}$ because the Eden growth process generates strands that compete with each other⁽²³⁾ and effectively mimic a quenched disordered environment.⁽⁵⁾ The exponents predicted from this value of H are shown in Table I. Figure 8 shows the log-log plot of $P(s, L)$ vs. s . The data points analyzed along the same lines as before, are consistent with the exponent τ of 1.40 which agrees with the scaling prediction (see Table I). It is remarkable that the self-similar and self-affine river network models yield very close predictions (indeed $d_I \sim 1.21$ whereas $2/(1 + H) = 6/5$) for all of the scaling exponents even though the underlying mechanisms are very distinct. We believe this point deserves further investigation.

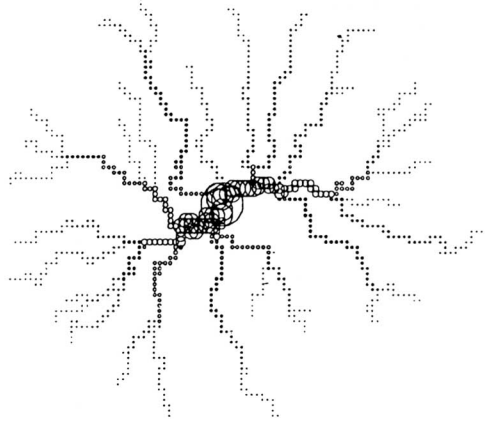


Fig. 7. Typical network of self-affine rivers flowing to an outlet in the center. The network has been obtained by generating an Eden growth process from a central seed and stopping the growth when the maximal horizontal distance reached is equal to 64 lattice constants. The size of the circles is a measures of s . Only sites with $s \geq 100$ are shown.

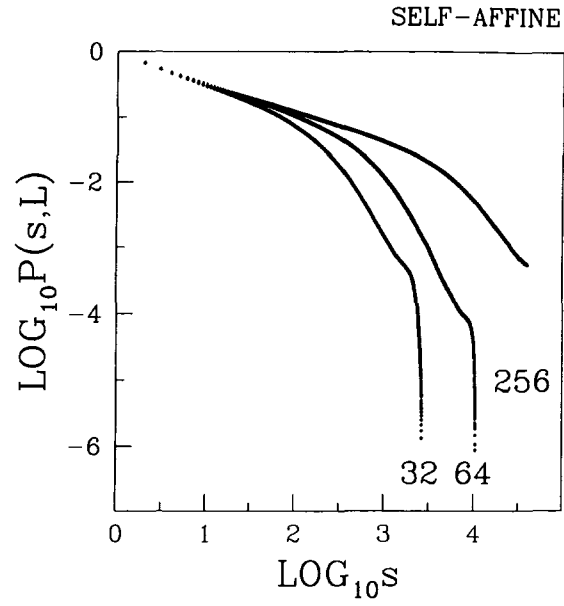


Fig. 8. A log-log plot of the cumulate area distribution $P(s, L)$ vs. s for the self-affine model. The system sizes are $L = 32, 64$, and 256 as indicated in the figure. The number of samples for the three cases are 1000, 500, and 200 respectively.

V. OBSERVATIONAL DATA

In this section we shall review some experimental known results to provide evidence that the two above toy models, albeit rather primitive, are in fact relevant in the interpretation of observational data. For a more exhaustive analysis see ref. 11.

The network associated with a given natural terrain pertaining to a river basin can be experimentally analyzed by using the so-called Digital Elevation Map (DEM) technique (see e.g., ref. 1 and references therein). In its digitized form, the elevation map of a terrain allows the determination of the soil height of areas (pixels) of order 10^{-2} Km². Thus a fluvial basin is represented in a objective manner over few (typically 3-4) log scales of linear size. A flowrate unit is associated with each pixel and the flow contributing to any pixel follows the steepest descent path through drainage directions. The resulting network (thus defined by the drainage directions) is therefore a two-dimensional representation of the three-dimensional landscape.

In Fig. 9 a representative network obtained in this fashion is shown. This particular network has the exponent $\tau = 1.40$ which is in very good agreement with both the self-similar and the self-affine models.

It is important to stress that the actual values of the critical exponents do vary from basin to basin. However, within each single river network, all

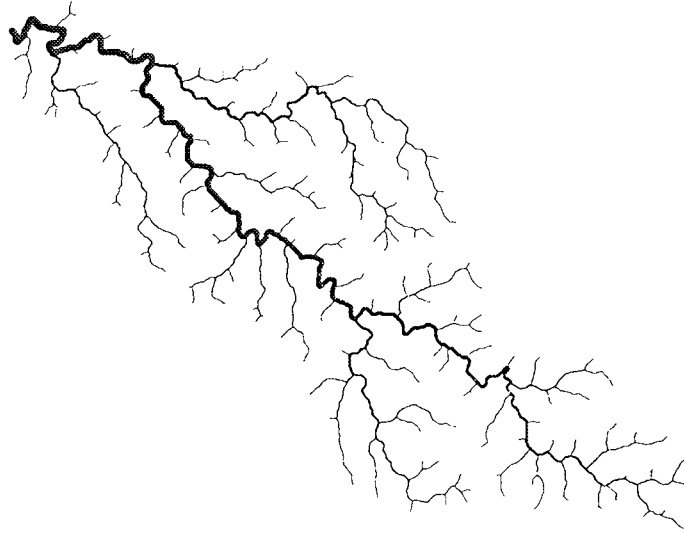


Fig. 9. The transportation network of the Johns river drainage basin in Kentucky, USA. Its extension is 984 Km². The measured exponents are: $\tau = 1.40$, $H = 0.67$.

the exponents closely satisfy the scaling relationships that we have derived. The exponent values for the network of Fig. 9 is in perfect agreement with our self-affine (Eden-like) model, although other networks often have slightly higher values of τ .⁽¹¹⁾

The measured values for d_I and H ranges between 1.02 and 1.07 and between 0.75 to 1.00 respectively.⁽¹¹⁾ The above models then lie at the outer edge of the observed data in both cases. We believe that although these two models do represent, at a very schematic level, two physical mechanisms occurring, at some length scale, in real rivers, our numerical results show that this is not sufficient and that other effect possibly combine to yield different numerical exponents.

As mentioned earlier, identical statistics can be obtained by using either self-similar ($d_I > 1$, $H = 1$) or self-affine ($d_I = 1$, $H > 1$) networks, provided that $d_I = (2/1 + H)$. In this respect a direct measure of the anisotropy of real rivers appears to be crucial.

Finally we remark that although the observational data favour self-affine rivers, the (statistical) similarity between each basin and its sub-basins, suggests that river networks are indeed self-similar, although their actual shape is anisotropic (as expected for a self-affine network).

VI. SUMMARY

We have studied two lattice models of spanning trees that lead naturally to fractal river networks. We have chosen a self-similar and a self-affine case on the basis that in nature there are features belonging to both characters, although it is commonly accepted that natural rivers are self-affine. The two models have very different physical motivations. The self-similar model is directly driven by disorder. Our choice of heterogeneities is spatially uncorrelated, and any degree of spatial correlation would decrease the small scale tortuosity of disorder-dominated paths. The resulting spanning tree-like structures exhibit a general similarity to river basins in overall appearance and very consistent scaling statistics. Our numerical results are consistent with previous estimates of the same model introduced on different physical grounds⁽¹⁰⁾ and corrects some misunderstandings present in the literature.⁽²⁾ More generally, our results show that fractal structures arise from the minimization of a disorder-dominated total energy functional and reinforce earlier suggestions⁽⁴⁾ on the connections of optimality with fractal growth. On the other hand the self-affine model has no disorder in the definition but it has buried in it a competition mechanism which *effectively* yields quenched disorder. Again our results are in accord with previous investigations but have broader consequences in our framework of analyzing the effects of heterogeneities on the networks.

Two recent investigations are pertinent to our work. In ref. 24 the interplay between quenched disorder and non-linearity in the landscape evolution was shown to be relevant for the interpretation of the real rivers field data. On the other hand, a even more recent renormalization group analysis of a continuum equation⁽²⁵⁾ suggests that the two disorder-dominated networks studied here, the unweighted spanning-trees studied in ref. 3 and the aforementioned landscape model of ref. 24, all belong to *different* universality classes albeit with very close exponents. We believe that this scenario is intriguing and deserves further attention.

ACKNOWLEDGMENTS

We are indebted to Deepak Dhar, S. S. Manna and Joachim Krug for useful discussions. This work was supported by grants from KBN (grant number 2P302-127), NASA, NATO and the Center for Academic Computing at Penn State.

REFERENCES

1. D. G. Tarboton, R. L. Bras, and I. Rodriguez-Iturbe, *Water Resour. Res.* **24**:1317 (1988); D. Lavallée, S. Lovejoy and D. Schertzer, *Fractals in Geography*, N. S. Lam and L. De Cola, eds. (Prentice Hall, Englewood Cliffs, 1993), 159; I. Rodriguez-Iturbe, M. Marani, R. Rigon, A. Rinaldo, *Water Resour. Res.* **30**:3531 (1994); D. R. Montgomery and W. E. Dietrich, *Nature* **336**:232 (1988); *Science* **255**:826 (1992); S. P. Breyer and R. S. Snow, *Geomorphology* **5**:143 (1992).
2. C. P. Stark, *Nature* **352**:423 (1991).
3. S. S. Manna and B. Subramanian, *Phys. Rev. Lett.* **76**:3460 (1996).
4. I. Rodriguez-Iturbe, A. Rinaldo, R. Rigon, R. L. Bras, E. Ijjasz-Vasquez, A. Marani, *Water Resour. Res.* **28**:1095 (1992); R. Rigon, A. Rinaldo, I. Rodriguez-Iturbe, E. Ijjasz-Vasquez, R. L. Bras, *Water Resour. Res.* **29**:1980 (1993); A. Rinaldo, I. Rodriguez-Iturbe, R. Rigon, E. Ijjasz-Vasquez and R. L. Bras, *Phys. Rev. Lett.* **70**:822 (1993); for earlier studies linking optimization principles to drainage networks, see A. D. Howard, *Water Res. Res.* **7**:863 (1971); **26**:2107 (1990) and references therein.
5. A. Maritan, F. Colaiori, A. Flammini, M. Cieplak and J. R. Banavar, *Science* **272**:984 (1996); F. Colaiori, A. Flammini, A. Maritan and J. R. Banavar, *Phys. Rev. E* **55**:1298 (1997).
6. Lattice models of river basin evolution are discussed, eg., by S. Kramer and M. Marder, *Phys. Rev. Lett.* **68**:205 (1992); R. L. Leheny and S. R. Nagel, *Phys. Rev. Lett.* **71**:1470 (1993).
7. T. Sun, P. Meakin and T. Jøssang, *Phys. Rev. E* **49**:4865 (1994); **51**:5353 (1995); *Water Res. Res.* **30**:2599 (1994); P. Meakin, J. Feder and T. Jøssang, *Physica A* **176**:409 (1991).
8. A. Maritan, A. Rinaldo, R. Rigon, A. Giacometti and I. Rodriguez-Iturbe, *Phys. Rev. E* **53**:1510 (1996).
9. J. R. Banavar, F. Colaiori, A. Flammini, A. Giacometti, A. Maritan and A. Rinaldo, *Phys. Rev. Lett.* **78**:4522 (1997).

10. S. S. Manna, D. Dhar and S. N. Majumdar, *Phys. Rev. B* **46**:4471 (1992).
11. R. Rigon, I. Rodriguez-Iturbe, A. Maritan, A. Giacometti, D. G. Tarboton and A. Rinaldo, *Water Resour. Res.* **32**:3367 (1996).
12. J. T. Hack, *U.S. Geol. Surv. Prof. Paper* **294**:1 (1957).
13. R. Chandler, J. Koplik, Lerman and J. Willemsen, *J. Fluid Mech.* **119**:249 (1982); R. Lenormand, *C. R. Seances, Acad. Sci. Ser. B* **291**:279 (1980).
14. See e.g., H. Takayasu, M. Takayasu, A. Provata and G. Huber, *J. Stat. Phys.* **65**:725 (1991).
15. A.-L. Barabasi, *Phys. Rev. Lett.* **76**:3750 (1996).
16. An optimal channel network is the spanning tree that minimizes $\sum_i P_i s_i^2$ where the sum over i runs over all the bonds of the tree, P_i is the erodability of the i -th bond and s_i is defined in Eq. (1). Our model corresponds to a heterogeneous basin with non uniform P_i and $\hat{\gamma} = 0$.
17. C. M. Newman and D. L. Stein, *Phys. Rev. Lett.* **72**:2286 (1994).
18. M. Cieplak, A. Maritan and J. R. Banavar, *Phys. Rev. Lett.* **72**:2320 (1994).
19. J. Feder, *Fractals* (Plenum, New York, 1988).
20. We are grateful to Deepak Dhar for correspondence on this point.
21. P. Meakin, *Phys. Scr.* **45**:69 (1992); P. Meakin, *J. Phys. A* **20**:L1113 (1987).
22. J. Krug and P. Meakin, *Phys. Rev. A* **40**:2064 (1989).
23. M. Cieplak, A. Maritan, and J. R. Banavar, *Phys. Rev. Lett.* **76**:3754 (1996).
24. G. Caldarelli, A. Giacometti, A. Maritan, I. Rodrigues-Iturbe and A. Rinaldo, *Phys. Rev. E* **55**:R4865 (1997); A. Rinaldo, I. Rodrigues-Iturbe, R. Rigon, E. Ijjazs-Vasques and R. L. Bras, *Phys. Rev. Lett.* **70**:822 (1993).
25. B. Tadic, *Phys. Rev. Lett.* (in press) (1997).